Available online at www.sciencedirect.com
SCIENCE DIRECT®
Applied Catalysis B: Environmental 50 (2004) 185–194
APPLIED CATALYSIS B: ENVIRONMENTAL
www.elsevier.com/locate/apcatb

The role of NO_2 and O_2 in the accelerated combustion of soot in diesel exhaust gases

Agus Setiabudi, Michiel Makkee*, Jacob A. Moulijn

Section Reactor and Catalysis Engineering, Faculty of Applied Sciences, Delft University of Technology, Julianalaan 136, NL 2628 BL Delft, The Netherlands

Received 20 April 2003; received in revised form 9 November 2003; accepted 19 January 2004

Available online 20 March 2004

Abstract

The role of NO_2 and O_2 in the combustion of soot was investigated by analysing the soot combustion characteristic and the DRIFT spectra of surface oxygen complexes (SOCs) as soot oxidation intermediates. It is found that in NO_2/O_2-soot, like in the CRT system, the oxidation of soot is initiated by the NO_2-soot reaction to create SOCs as intermediates. O_2 reacts with SOCs, eventually yielding CO and/or CO_2. This mechanism results in a higher oxidation rate when NO_2-soot reaction occurs in the presence of O_2. The potential of using Printex-U, a flame soot, in exploratory diesel soot combustion studies is discussed. It is concluded that in general this is the case except for the fact that real soot can contain adsorbed hydrocarbons that will increase the reactivity of the soot in the absence of NO_2.

Keywords: Diesel soot; Soot oxidation mechanism; NO_2; Continuously regenerating trap; CRT; DRIFT spectra of soot

1. Introduction

Diesel engine emissions have gained considerable attention due to their health risk and environmental concerns, especially particulate matter and NO_x. These components are considered to be the main pollutants of diesel engine emissions together with CO and HC. Particulate matter is composed of aggregated carbonaceous soot and adsorbed hydrocarbon, which might be often very toxic. Currently, diesel oxidation catalysts (DOCs) are applied to oxidise CO and (adsorbed) HCs to CO_2. The two remaining main pollutants (soot and NO_x), regulation is in force and more stringent regulation will be effected in the near future. Therefore, a lot of effort is being put on the development of catalytic diesel soot filter as well as of NO_x abatement technologies.

The so-called continuously regenerating trap (CRT) is an example of one of diesel particulate abatement systems. This CRT system shows an excellent performance during a road test over 700,000 km in the presence of ultra-low sulphur diesel fuel [1]. The CRT system combines trapping of soot in a wall-flow monolith, and two chemical processes, i.e., platinum catalysed NO oxidation to NO_2 and the subsequent oxidation of trapped soot with the NO_2 produced. Platinum catalyst also functions as an oxidation catalyst for CO and HC oxidation. A successful CRT application demands sufficient NO_2 production capacity and an optimal usage of NO_2. The exhaust temperature has also to be high enough for the reaction to take place at the required rate. Satisfactory operation has been reported at exhaust temperature exceeding 570 K [2]. PSA-Peugeot and Toyota have also introduced their after-treatment system with different reactions and operational systems [3,4]. The PSA-Peugeot is commercially introduced (more than 500,000 unit are in the market; end 2003), whereas Toyota is in its demonstration phase.

The reaction of soot with NO_2 has been studied extensively, mainly in order to explain the processes taking place in the atmosphere [5,6]. The reaction does not lead to the formation of CO and NO as taken place in the CRT, but more on the reaction of NO_2 and H sites of the soot to form HONO. It is, therefore, not surprising that the kinetic regime usually studied is far from that under realistic conditions as occurring in the after-treatment system of a diesel engine. Recently, a study has been conducted to extract the kinetics of the reaction of NO_2 with carbon black in the presence of O_2 and H_2O in a temperature range relevant to the CRT system [7]. Gray et al. studied the dynamics of NO_2 and

* Corresponding author. Tel.: +31-15-2781391; fax: +31-15-2785006.
E-mail address: m.makkee@tnw.tudelft.nl (M. Makkee).

0926-3373/$ – see front matter © 2004 Elsevier B.V. All rights reserved.
doi:10.1016/j.apcatb.2004.01.004

carbon reaction gravimetrically over the temperature range of 423–623 K [8]. Using carbon black to represent diesel soot, Lur'e and Mikhno [9] indicated that the activation energy of the initial stage of the main NO_2 oxidation of soot is 50 kJ/mol at temperatures between 475 and 625 K. The NO_2–graphite reaction has also been studied between 675 and 995 K by scanning tunnelling microscopy [10].

In this present study the reactivity of two realistic diesel soot and a flame soot to O_2 and NO_2 are examined. The role of NO_2 and O_2, both individual and the mixture thereof, in the oxidation of soot are emphasised. Printex-U, the flame soot, has been chosen as a soot model, since this model soot has been used to substitute diesel soot in soot-O_2 reaction researches for more than a decade [11,12]. In view of the high practical interest, it is important to validate Printex-U as a diesel model soot in NO_2-soot based reaction in particular in CRT-related studies. The role of oxygen in the NO_2-assisted soot oxidation was studied by correlating the flow-reactor experiment with the DRIFT analysis of soot oxidation intermediates.

2. Experimental procedure

2.1. Material

A soot model and two types of realistic diesel soot samples have been studied. The soot model is Printex-U, a gift from Degussa. The diesel soot samples were produced from a state-of-the-art modern common-rail diesel engine, which operated at idle or full load conditions. Diesel soot produced at idle conditions is referred to as 'idle soot' and the one produced at full load condition as 'full load soot'. These two soot samples represent diesel soot that is normally produced in the real life diesel engine operations.

Throughout this paper, the term soot refers to as 'as received soot', unless otherwise stated. The physical characteristics of the samples, elemental analysis, and BET surface area, are given in Table 1. In the elemental analysis, the samples were combusted in oxygen up to 1273 K. The gaseous products were flushed with He carrier through the reducing reactor, so the emerging gasses were only CO_2, SO_2, N_2, and H_2, that were quantified by gas chromatography. The balance component is thought to be oxygen as oxygen containing hydrocarbon compounds. BET surface area was measured by a volumetric N_2 physisorption at 77 K. The sample was dried overnight at 373 K, of which its weight was used in the calculation. XRF analysis indicates the presence of iron, aluminium, calcium, sulfur, and phosphor as the main elements in the ash.

The experimental works consisted of thermo-gravimetric analysis (TGA), the temperature programmed oxidation (TPO in a flow reactor) and diffuse reflectance infrared Fourier transformed (DRIFT) analysis coupled with mass spectrometry experiments. The purpose of the TG analysis experiments were to determine the fraction of volatile material present in the soot samples, the reactivity of the soot samples to O_2, and the influence of ageing in an inert gas (helium) on the reactivity soot. In the flow reactor experiments (TPO) the reactivity of as received and aged soot samples to NO_2 and O_2 and the mixture thereof were explored. Ex situ DRIFT experiments were performed to analyse the soot oxidation 'intermediates'. The intermediate was prepared in the flow reactor by partly reacting soot samples with individual reactant gas(ses), NO_2 and O_2, and the mixture thereof. The following paragraph describes each experimental procedure in more detailed.

The apparatus for thermo gravimetric analysis was a TGA/SDTA 851^e from Mettler Toledo. The sample is placed in an aluminum crucible with a content of 70 μl. The oven can be operated in a temperature-programmed mode, while simultaneously the weight of the sample and the heat flux of adsorption or desorption can be measured. Every soot samples were heated from room temperature to 823 K at 1.5 K/min heating rate with 100 ml/min He flow and 100 ml/min synthetic air, respectively. The soot samples treated with He is referred to as 'aged soot'. These aged soot samples were further used in TGA analysis with synthetic air and in a flow reactor for the TPO experiment with O_2.

The reactivity of soot samples with individual O_2, NO_2, and the mixture thereof were tested in a flow reactor set-up. The simplified flow scheme of the equipment is shown in Fig. 1. The feed gasses used were nitrogen dioxide and argon as a gas balance. With the exception of oxygen, which is injected just upstream of the reactor, all gasses are mixed in the mixing section.

In every experiment, 10 mg soot was diluted by 400 mg SiC and placed into a 7-mm diameter quartz reactor tube. The purpose of SiC is to avoid possible soot sample agglomeration and to prevent a temperature run-a-way in the reactor bed during the oxidation process. Table 2 summarises the gas compositions used with Ar as balance gas. The sample was heated at 0.2 K/min to 900 K, while a Hartman & Braun Uras 10E Non-Dispersive Infra-Red analyser (NDIR) was used to analyse CO, CO_2, NO, and SO_2. A NO_x analyser, CLD 700 EL ht from Eco physics, is placed downstream of

Table 1
BET surface area and elemental composition of the soot samples

Sample	BET surface area (m^2/g)	C (w/w, %)	H (w/w, %)	N (w/w, %)	S (w/w, %)	Ash (w/w, %)
Idle soot	<5	70.80	3.85	1.16	0.48	3
Full load soot	18 (±1)	68.95	1.40	1.11	0.63	6
Printex-U	95 (±1)	91.24	0.52	0.17	–	–

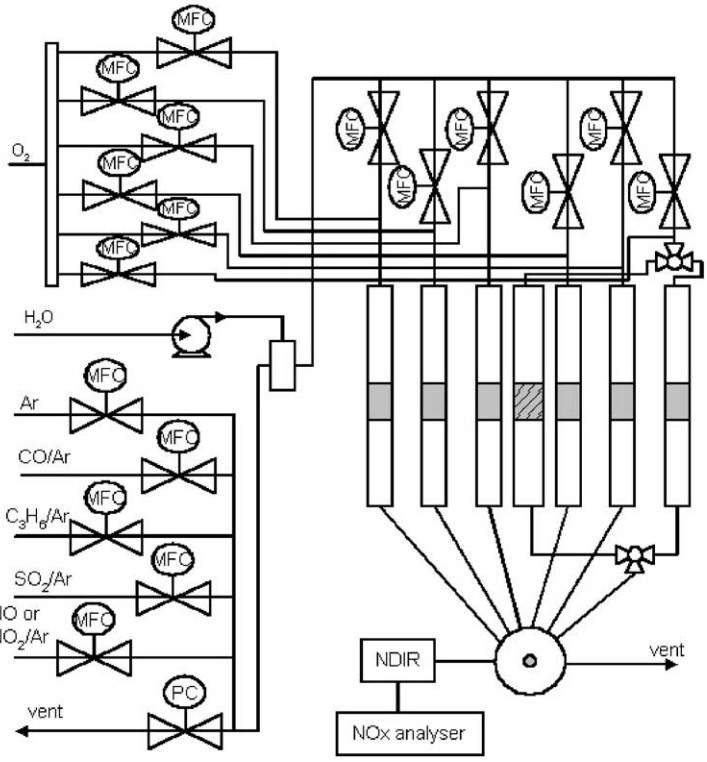

Fig. 1. Simplified flow reactor equipment.

the NDIR to analyse NO and NO_2. The mass balance for soot oxidation was calculated by integrating the amounts of CO and CO_2 released during reaction. Data on CO and CO_2 can be calculated and the sum of the two is presented as the soot oxidation rate.

As mentioned DRIFT spectroscopy analysis were performed to identify the intermediates formed in the oxidation of soot with NO_2. Prior to sample analysis, Printex-U was pre-treated in the flow reactor equipment. Printex-U was exposed to several gas mixtures in the flow reactor. For NO_2 and NO_2/O_2 exposures, 200 ml/min gas stream containing 500 ppm NO_2 and 500 ppm NO_2 + 10% O_2, respectively, were used at 625 K. To reach similar conversion levels the contact time with 500 ppm NO_2 was 6 h, while with 500 ppm NO_2 + 10% O_2 this was 4 h. The conversion level of soot during this preparation procedure is 40–50%. A higher temperature, around 700 K, was used for the exposure with O_2 in order to reach a comparable reactive interaction. The spectrum of fresh Printex-U was also measured for comparison.

Table 2
Scheme of gas composition used in the flow reactor experiments

Soot sample	NO_2 (ppm)	O_2 (%)			
Idle soot		0	2	10	15
	500	X	–	X	–
	0	–	–	X	–
Full load soot	500	X	–	X	–
	0	–	–	X	–
Printex-U	500	X	X	X	X
	0	–	–	X	–
Aged soot	0	–	–	X	–

X: compositions used.

The analysis of soot oxidation intermediates by means of DRIFT spectroscopy was done ex-situ. The efforts to performed in-situ experiment to produce intermediates from the reaction of NO_2 and O_2 with soot failed due to (1) almost complete IR light absorption by an almost completely black body of soot materials, and (2) the general used diluent KBr will react with NO_2 [13]. Also the usage of other IR-diluents like SiO_2 and SiC failed.

After the preparation in the flow reactor, the NO_2, NO_2/O_2, and O_2-exposed Printex-U samples were diluted with KBr for about 1:100 mass ratio. A Nicolet Magna 850 spectrometer with a DTGS detector and a Spectratech diffuse reflectance accessory equipped with a high temperature cell was used. The samples were placed in the DRIFT reactor cell coupled to a mass spectrometer (Thermostar^{TM} from Pfeiffer Vacuum). The reactor cell scheme is presented in Fig. 2. DRIFT spectra of both the background (only KBr) and the KBr-exposed Printex-U were taken at room temperature, 523, 623, and 723 K under He. The emissions of mass 28, 30, 44, and 46, attributed to NO, CO, CO_2, and NO_2, respectively, were monitored by mass spectrometry. All spectra were recorded by collection of at 124 scan with a resolution of 8 cm^{-1}. It should be noted that during the quenching of the soot samples and the transfer of the

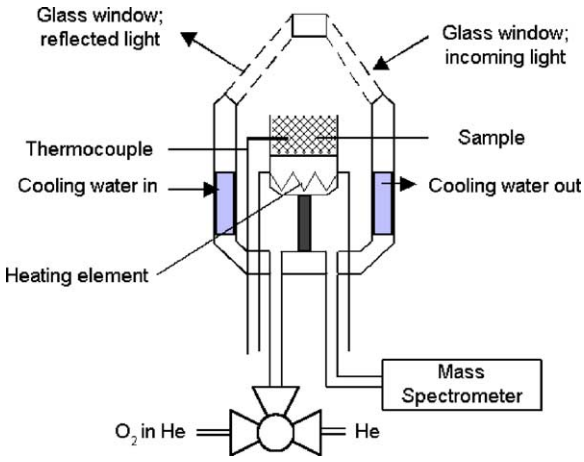

Fig. 2. In situ DRIFT reactor cell.

pre-treated soot samples from the flow-reactor set-up to the DRIFT cell some of the intermediate might still decompose. This decomposition can be probably neglected since there is no sign of inhibition in the isothermal soot oxidation when the feed to reactor is switched from 10% oxygen to complete argon (no oxidation is observed) to 10% oxygen. In the last step of this step-response procedure the oxidation rate is identical to the oxidation rate as in previous step when 10% oxygen was present. At the same time all soot mass balances were closed.

3. Results

3.1. Reactivity of soot to O_2 and NO_2

TGA experiments of soot samples in inert atmosphere provide information on the amount of volatile materials adsorbed on primary soot particles. In Fig. 3, the solid lines represent the data. Upon heating to 823 K, reductions of samples mass were observed, i.e., about 50% for idle soot, 20% for full load soot, and only 4% for Printex-U. The mass reduction for idle soot starts already at 400 K, while for full load soot it occurs at 600 K. This data correlate with the hydrogen content, as listed in Table 1; the higher the H-content, the higher the mass loss.

In synthetic air, the weight losses profiles are significantly different. The dash lines in Fig. 3 show these. It has to be noted that the weight loss is a simultaneous effect of volatilisation, reactive gas adsorption, and oxidation. At low temperature the trends of Printex-U and full load soot are similar to those observed in He. For idle soot, up to 580 K the sample weight decreases slower than that in He. At higher temperature, where soot oxidation expectedly takes place, the weight loss decreases much faster in air than that in He.

The reactivity of soot samples with respect to O_2, NO_2, and NO_2/O_2 analysed in the flow-reactor with TPO techniques are shown in Fig. 4. With O_2 as oxidising agent,

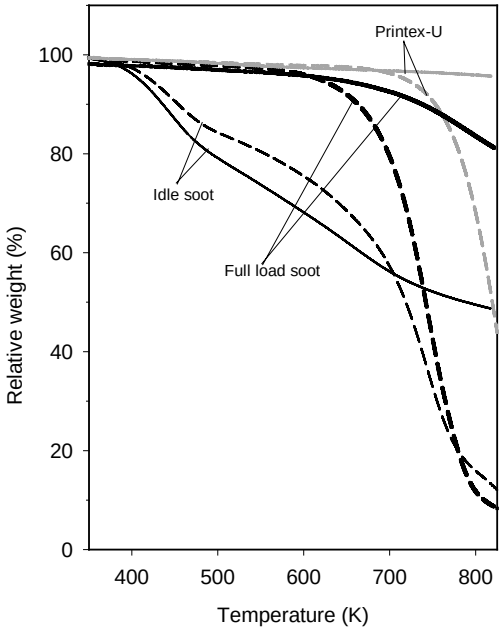

Fig. 3. TG profile of soot samples treated in He (solid line) and synthetic air (dash line).

Fig. 4a, each sample is oxidised in a different temperature region. The sequence is idle soot < full load soot < Printex-U. It is interesting that in idle soot a shoulder around 550 K is observed. It has to be noted that each soot sample was completely oxidised during the TPO in O_2; for idle and full load the combustion is completed at 800 K, while for Printex-U complete combustion was achieved at 900 K.

With NO_2 as oxidising agent, all soot samples show similar reactivity as indicated by comparable oxidation profile among all samples, see Fig. 4b. Compared to the reactivity in O_2, in NO_2 the samples are more reactive. Idle soot shows once again a shoulder, but at a lower temperature (around 500 K) compared to that observed in O_2. Its oxidation rate increases slightly slower than those of two other samples. Its combustion is ended at slightly higher temperature.

In a mixture of NO_2 and O_2 the oxidation profiles shift further to a temperature lower than in NO_2 or O_2. Up to 500 K the profiles are identical, but idle soot is less reactive at higher temperatures. In all cases idle soot shows the lowest oxidation rate.

To evaluate the effect of O_2 further, experiments were done in various O_2 partial pressures, while keeping the amount of NO_2 constant. For this purpose only Printex-U as the soot sample is illustrated. The results are shown in Fig. 5. The two other soot samples (idle and full load) showed identical spectral changes as function of the oxygen partial pressure (not shown). Clearly, the presence of 2% O_2 already shifts the oxidation profile to significantly lower temperatures. At higher O_2 partial pressure no additional shift was observed.

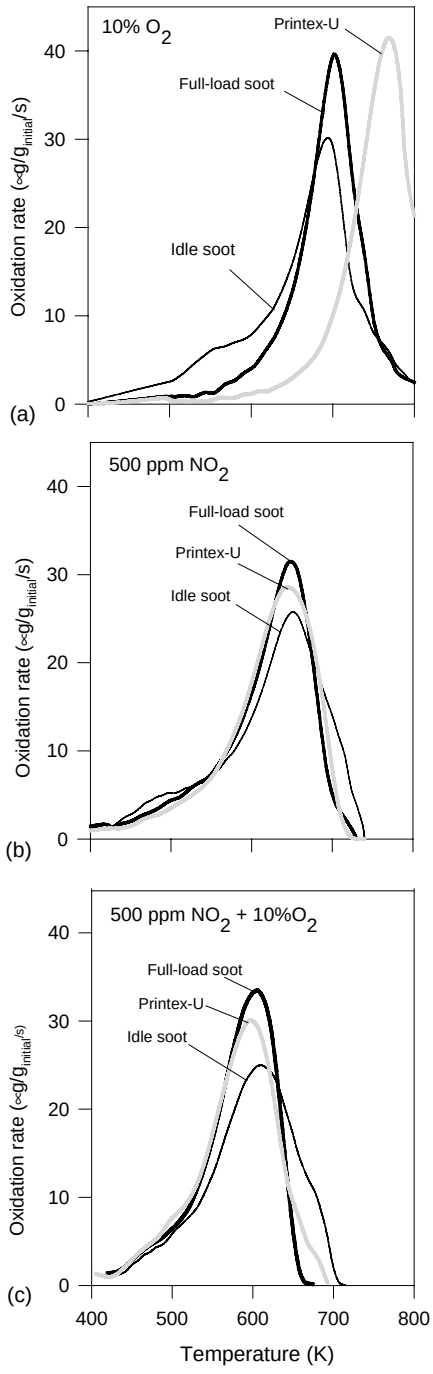

Fig. 4. TPO profile of soot samples measured in flow reactor with: 10% O_2 500 ppm NO_2 500 ppm $NO_2 + 10\%$ O_2.

Aged soot samples, that had lost their volatile material during heating with He, were analysed further by TGA in synthetic air. The results are shown in Fig. 6. The results of the as received soot (dash lines) are also incorporated in the figure for comparison. It can be seen that aged idle soot shows a TG curve that is dramatically different from that of the as received one, while for full load soot and Printex-U, the effect of temperature ageing is insignificant. At low temperature, a weight increase is observed in aged

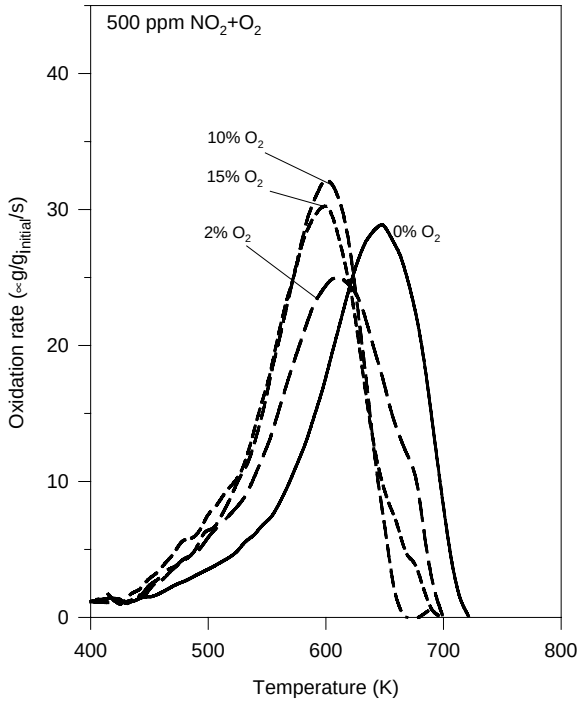

Fig. 5. Effect of O_2 partial pressure on the soot oxidation profile in $NO_2 + O_2$ reaction system.

idle soot. After about 25% conversion the curves for idle soot and full load soot are essentially identical.

In Fig. 7 the TPO curves for aged soot are compared with those of the as received analogues. As can be seen in Fig. 7a, aged idle soot obviously decreases its reactivity and the low-temperature shoulder has disappeared. Aged full load soot does not differ much from as received sample,

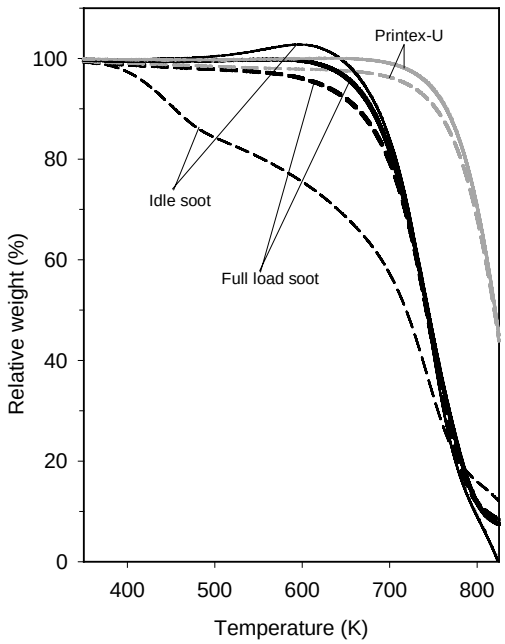

Fig. 6. TG profile of as received soot (dash line) and aged soot sample (solid line) treated with synthetic air.

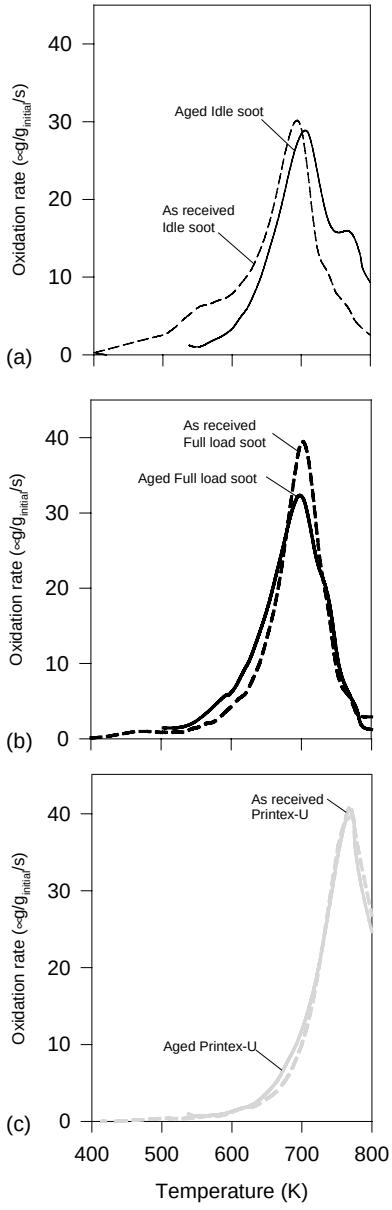

Fig. 7. TPO profile of as received soot (dash line) and aged soot sample (solid line) measured in flow reactor with 10% O_2: (a) idle soot, (b) full load soot (c) Printex-U.

while on Printex-U ageing hardly shows any influence, as shown in Fig. 7b and c, respectively.

3.2. DRIFT spectra of O_2, NO_2, and NO_2/O_2-exposed Printex-U, and its decomposition product

To identify the role of NO_2 and O_2 in the soot-NO_2–O_2 reaction system, the O_2, NO_2, and NO_2/O_2-exposed at elevated temperatures Printex-U samples were heated in He while their DRIFT spectra and gas emissions were recorded simultaneously. The spectra are presented in Fig. 8. The spectrum of untreated Printex-U is incorporated for comparison. Typical wave numbers of carbon–oxygen complexes, taken from literatures [14–16], are summarised in Table 3 and indicated in Fig. 8. These complexes are located at (1) 1810–1665 cm^{-1}, (2) 1650–1500 cm^{-1}, and (3) 1350–1200 cm^{-1}. It is shown that a very low intensity of carbon–oxygen complexes have already existed on untreated Printex-U. Printex-U that had been exposed to O_2, Fig. 8a, shows three broad peaks in the ranges indicated for the carbon–oxygen complexes with moderately higher intensities than those of the untreated Printex-U. It has to be noted that these broad peaks composed of many carbon oxygen functionalities. Therefore, it is not possible to assign its individual vibration mode. When the spectra were measured at stepwise to higher temperatures, a gradual decrease of absorbances located at 1810–1665 cm^{-1} was observed, while two other bands does not change much.

Fig. 8b represents the spectra of NO_2-exposed Printex-U. In contrast to those for O_2 atmosphere the spectra are different in all three ranges; the peak located between 810 and 1665 cm^{-1} is higher and the peak located between 1650 and 1500 cm^{-1} is broader. In the spectrum measured at room temperature double peaks located at 1610 and 1550 cm^{-1} are observed. In the complex region of 1350–1200 cm^{-1}, a peak originated from 1210 cm^{-1} contributes to the spectrum, which is not the case for O_2-exposed Printex-U. Upon heating in inert atmosphere the peak located between 1810 and 1665 cm^{-1} decreases more rapidly than that of the O_2-exposed peaks. At 723 K the double peak located at 1650–1500 cm^{-1} reduces to one broad band. Furthermore, the peak originated from 1210 cm^{-1} does not exist anymore. Negative absorbances at 1380 cm^{-1} are observed particularly at 623 and 723 K.

When Printex-U was exposed to the mixture of 500 ppm NO_2 + 10% O_2, the pattern shows similar characteristic to that of O_2-exposed and NO_2-exposed ones. An interesting feature is the peak located at 1810–1665 cm^{-1}, which is higher than the O_2-exposed but lower than the NO_2-exposed one. No double peak is observed in the region of 1650–1500 cm^{-1} and neither the 1210 cm^{-1} peak. Negative absorbances are again observed.

The emission of mass 28, 30, 44, and 46, attributed to CO, NO, CO_2, and NO_2, respectively, following heating in He of O_2, NO_2, and NO_2/O_2-exposed Printex-U, are presented in Fig. 9. The dotted lines indicate the points when stepwise heating was started. It has to be noted that a rapid heating mode was used. The heating step took less than 1 min. In O_2-exposed Printex-U hardly any emissions of gas following heating is observed. Contrary, the soot sample that had been exposed NO_2, emitted a small amount of CO, CO_2, and NO already at 523 K. For CO_2, the emission is very fast during the heating up to higher temperature, it reaches a maximum and decreases slowly. For NO_2/O_2-exposed Printex-U only emissions of CO_2 are clearly detected, at a lower intensity than that for NO_2-exposed Printex-U. Together with CO, NO, CO_2, and NO_2 the emission of 28 amu, which can be ascribed besides to CO also to N_2, was also measured, but no such emission was observed.

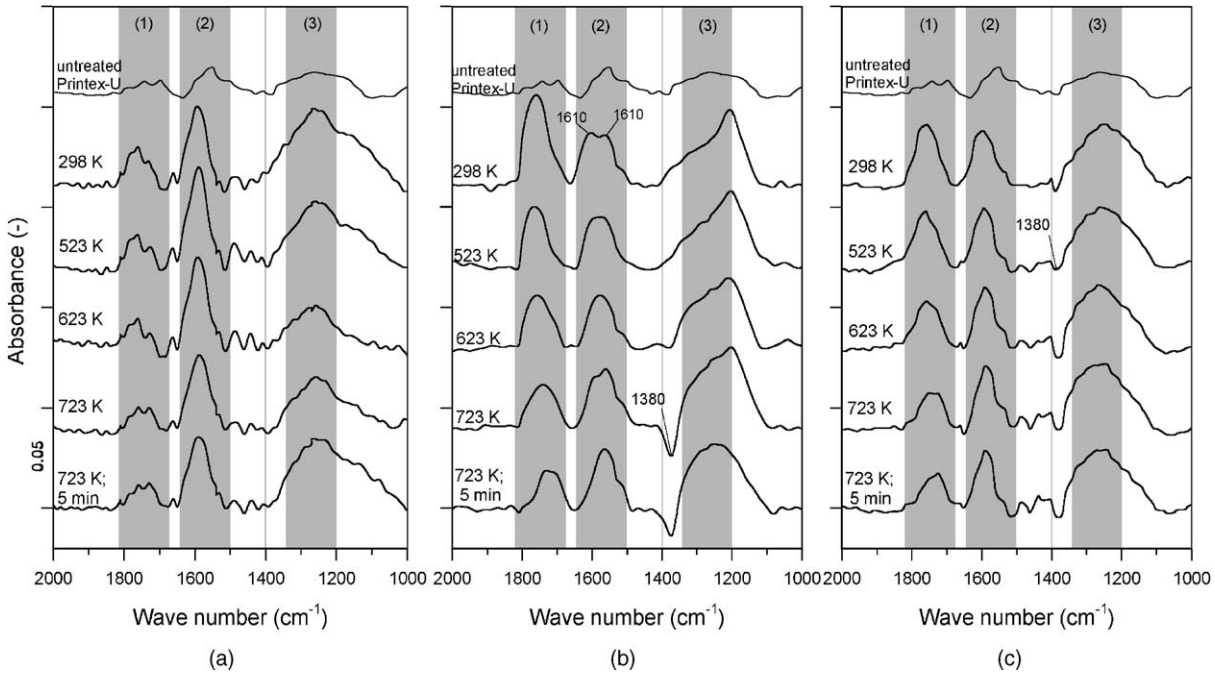

Fig. 8. DRIFT spectra of exposed Printex-U step wisely heated in He: (a) O_2-exposed (b) NO_2-exposed (c) $NO_2 + O_2$-exposed Printex-U.

Table 3
Summary of surface oxygenated carbon complexes and its IR assignments

Structure [15]	Functionality	Decomposition product	IR assignment region [11–13]		
			1810–1665 cm^{-1}	1650–1500 cm^{-1}	1350–1220 cm^{-1}
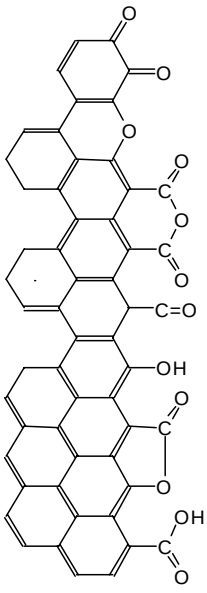	Quinone	CO		1590 (C=C)	
	Ether	CO			1200–1275 (C–O–C)
	Anhydride	$CO + CO_2$	1776, 1835 (C=O)		1210–1310 (C–O)
	Cabonyl	CO	1635 (C=O)		
	Phenol	CO			1230 (C–O) 1310 (O–H)
	Lactone	CO_2	1765–1745 (C=O)		1160–1370 (C–O)
	Caboxylic	CO_2	1665–1720 (C=O)		1120–1200 (C–O)

4. Discussion

4.1. Reactivity of soot to O_2 and NO_2, TPO

Depending on engine operation modes, a complex mixture of partially burned and unburned fuel and of lubricating oils is normally bounded to the particles emitted from diesel engine. The compounds are normally high- and intermediate-molecular weight compounds, known as soluble organic fraction (SOF). Compared to the primary soot particle, which is mainly composed of elemental carbon, these adsorbed hydrocarbon compounds are easier to oxidise.

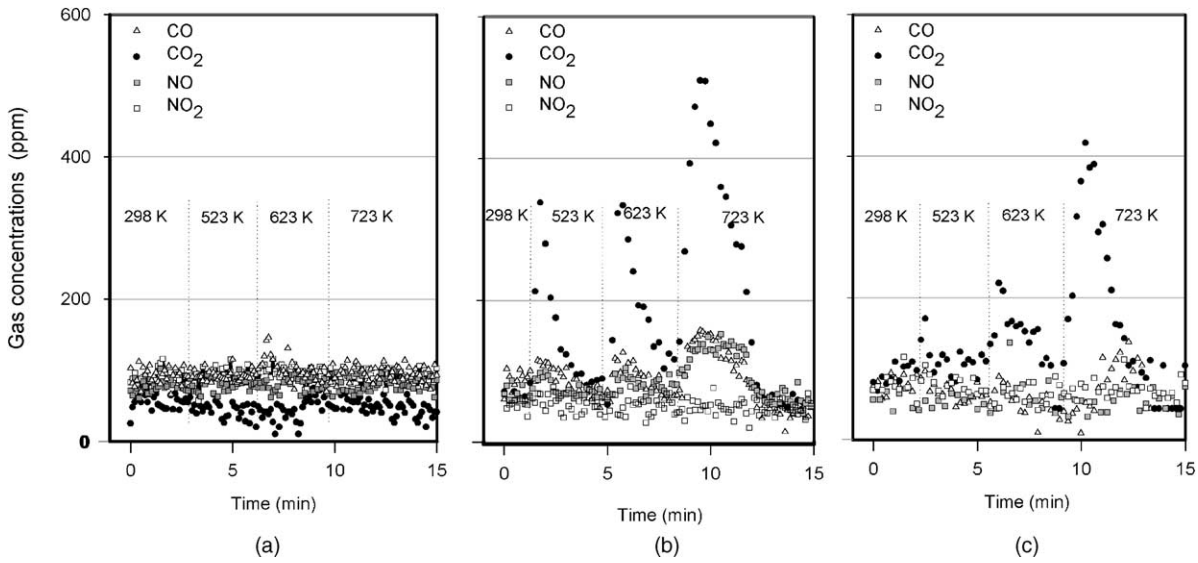

Fig. 9. Mass spectrometry of exposed Printex-U heated in He: (a) O_2-exposed (b) NO_2-exposed (c) $NO_2 + O_2$-exposed Printex-U.

Hydrocarbon analysis of adsorbed diesel particulate matter requires a complex procedure especially when identification of the individual components is desired. Fortunately, the hydrogen content roughly indicates the fraction of adsorbed hydrocarbon. The hydrogen content shown in Table 1 increases in the order of Printex-U < full load soot < idle soot. This is in good agreement with the TGA results, which show that the amount of volatile material follows the same order. This result physically makes sense since idle soot was produced from a low-load engine operation, full load soot from high-load engine operation, and Printex-U is a flame-soot produced by high-temperature pyrolysis.

When TGA is performed in air the initial weight loss of idle soot is slower than that in He. At first sight this might seem surprising. The explanation comes from an analysis of the three possible processes that might take place simultaneously, viz. volatilisation of hydrocarbon, gas adsorption, and soot oxidation. It is concluded that O_2 chemisorption is responsible, and possibly also desorption of hydrocarbons interferes.

The presence of adsorbed hydrocarbon in the diesel soot clearly affects its reactivity to O_2. Idle soot that contains most adsorbed hydrocarbons ignites at lower temperature than the two other samples. The shoulder at 550 K confirms that part of the adsorbed hydrocarbon is more reactive to O_2. In this way ignition of the soot particles takes place. The less quantity of hydrocarbon in Printex-U explains its less reactivity to O_2.

An interesting result is shown by aged idle soot in the TGA experiment when heated with air, as shown in Fig. 6. It is clearly observed that up to 600 K instead of a weight loss, a weight gain is observed. Oxygen chemisorption could again explain the behaviour. This phenomenon is characteristic for coal combustion where the same explanation was reported [17]. The second interesting behaviour of aged idle soot is its TG profile during the combustion stage, which is very close to that of as received full load soot. In TPO experiments again this same behaviour was observed. The relevance of this phenomenon is that in a real diesel exhaust systems the characteristics of soot produced in low-load operation can change to full-load characteristics, for example when soot, produced under low-load conditions is trapped on the filter and experiences heating without being combusted.

The TPO experiment performed with 500 ppm NO_2 shows a significantly different oxidation curve from that of O_2. The reactivity for all soot samples to NO_2 is almost identical. The effect of adsorbed hydrocarbon has disappeared except for a very weak shoulder in the case of idle soot. When O_2 is added to 500 ppm NO_2, the soot oxidation rates increase. This effect is beneficial for application of C–NO_2 based reactions filter regeneration, because 5–15% O_2 is always presents in the exhaust gas. The role of O_2 in the mechanism of soot oxidation in the presence of NO_2 and O_2 will be discussed in the next section based on literature study and DRIFT spectra of treated soot samples (intermediates) and mass spectrometry of emitted reaction product.

4.2. DRIFT analysis of O_2, NO_2, and NO_2/O_2-exposed soot, formation and decomposition of SOCs

The soot oxidation products, CO and CO_2, are the results of intermediates decomposition. They are, in principle, various carbon–oxygen functionalities formed on the surface of carbon particles. Throughout this paper the intermediates are named surfaces oxygen complexes (SOCs). Upon heating, SOCs decompose by releasing CO and/or CO_2. Depending on the type of carbon functionality, SOCs decomposition takes place at different temperatures. Figueiredo et al. [18] summarised the decomposition temperature in TPD of carbon functionalities and their decomposition product. Table 3

summarises the complexes and their products, together with the IR assignments [14–16].

The fact that many functional groups give bands in close ranges explains the appearance of the broad bands. Therefore, it is not possible to specify the functional groups individually. The DRIFT spectra of SOCs at 298 K, Fig. 8a and b, confirm that both O_2 and NO_2 are able to produce intermediates as shown by higher SOCs spectra intensities compared to that of untreated Printex-U. Both gasses produce similar oxygen containing functional groups. It is concluded that NO_2 produces more carboxylic, lactone, and/or anhydride than O_2 as shown by higher peak located at 1810–1665 cm^{-1}. This is in agreement with the observation that the reactivity of NO_2 to soot is higher compared to that of O_2. The double peak at 1610 and 1540 cm^{-1}, observed only on NO_2-exposed Printex-U, can be attributed to the formation of C–NO_2 functionality. In literature R-NO_2 is assigned at 1540 and 1340 cm^{-1} [14,19]. The 1340 cm^{-1} peak cannot be clearly seen in the spectra, probably because of interference with other oxygenated carbon functionality at the region. The 1210 cm^{-1} wave number should not be related to the R-NO_2 functionalities. It is attributed to SOCs. Since this peak disappeared upon heating (no NO_2 emission is observed as can be seen in Fig. 9b), it is concluded that it originates from unstable complexes. We tentatively conclude that lactones are responsible. The negative absorbance at 1380 cm^{-1} is probably caused by the background correction; but its origin is still largely discussed in the open literature.

When Printex-U was exposed to the NO_2/O_2 gas mixture, the intensities of SOCs assignments are lower than that of the one exposed to NO_2. This can be explained as follows. Considering the reactivity of NO_2, which is much higher than O_2, it suggests in itself that in NO_2/O_2 gas mixture the oxygenated carbon complexes were firstly formed from the reaction of Printex-U with NO_2. It should be noted that the exposure of Printex-U by the gas mixture took place at 625 K, where oxidation with O_2 is not significant. So, the role of O_2 in increasing the oxidation rate in the presence of NO_2 should not be related with the formation of additional SOCs. During the exposure of soot with NO_2/O_2 mixture, O_2 is present abundantly in comparison to NO_2, and, as a consequence, it reacts with the complexes formed by NO_2. O_2 might react with less oxygenated carbon, like aldehyde or ketone to a higher oxygenated complex such as carboxylic or lactone that are easier to decompose. Another possibility is the reaction of O_2 with the complexes to form CO or CO_2 directly. Another feature of NO_2/O_2 exposed soot compared to the NO_2 one is the R-NO_2 peak that is not observed in NO_2/O_2 exposed Printex-U. The reaction of surface R-NO_2 with O_2 during the SOCs formation might explain the phenomena.

The reasoning can be summarised as follows. Although diesel soot normally contains oxygen complexes but these are unreactive to O_2. Due to its reactivity, NO_2 initiates the creation of O-containing sites intermediates, SOCs, which are more reactive than the complexes that have already existed. As a consequence, O_2 is able to react with them. This reasoning is strictly analogous to the modelling work of Chen et al. [20].

In the following the NO_2/O_2-soot reaction phenomena are discussed based on reaction mechanism schemes. As basis, the generally accepted reaction scheme for the oxidation of carbonaceous material is used [20–23]. In the NO_2/O_2 mixture the formation of SOCs is initiated by NO_2, the reactions are described as:

$$CC_f + NO_2 \rightleftharpoons CC_f\{O\} + NO \quad (1)$$

$$CC_f\{O\} + NO_2 \rightleftharpoons C\{O\}C_f\{O\} + NO \quad (2)$$

CC_f indicates the free carbon atom, $CC_f\{O\}$ and $C\{O\}C_f\{O\}$ both represent SOCs, while $\{O\}$ indicates an oxidised carbon. The last species, $C\{O\}C_f\{O\}$, is considered to be relatively unstable of which CO and CO_2 might be produced. Reaction (1) can occur with O_2 only at relatively high temperature. In the NO_2/O_2 mixture the formation of $C\{O\}C_f\{O\}$ can also take place with O_2 through:

$$CC_f\{O\} + \tfrac{1}{2}O_2 \rightleftharpoons C\{O\}C_f\{O\} \quad (3)$$

SOCs decomposition can occur through thermal dissociation of intermediates:

$$CCC_f\{O\} \rightarrow CC_f + CO \quad (4)$$

$$CC\{O\}C_f\{O\} \rightarrow CC_f\{O\} + CO \quad (5)$$

$$CC\{O\}C_f\{O\} \rightarrow CC_f + CO_2 \quad (6)$$

or through the reaction with O_2 and NO_2:

$$CCC_f\{O\} + \tfrac{1}{2}O_2 \rightarrow CC_f + CO_2 \quad (7)$$

$$CC\{O\}C_f\{O\} + \tfrac{1}{2}O_2 \rightarrow CC_f\{O\} + CO_2 \quad (8)$$

$$CCC_f\{O\} + NO_2 \rightarrow NO + CC_f + CO_2 \quad (9)$$

$$CC\{O\}C_f\{O\} + NO_2 \rightarrow NO + CC_f\{O\} + CO_2 \quad (10)$$

In the genesis of SOCs with NO_2/O_2 mixture, O_2 is present abundantly in comparison to NO_2. So, among reaction (7) to (10), reaction (7) and (8) will dominate the reactions [21]. According to the reaction scheme, O_2 plays a role in the formation of less stable complexes, reaction (3), and in the decomposition of SOCs, reactions (7) and (8).

The mass spectrometry data shows extended evolution of CO and CO_2 from NO_2-exposed Printex-U when heated under He, as shown in Fig. 9b. This is in agreement with the decrease of the 1800–1665 cm^{-1} peak bands observed in DRIFT spectra, as shown in Fig. 8b. This suggests that carboxylic acid and/or lactone are the major species responsible for the CO and CO_2 formation. The fast decrease of the CO_2 mass spectrometry signal to the background level at every step of temperature indicates the variety of limited stability of the SOCs as a function of temperature. The fact that exposure of NO_2/O_2 to Printex-U yields relatively low amounts of CO and CO_2 compared to that of NO_2-exposed Printex-U is in agreement with this model.

In NO_2-exposed Printex-U the emission of CO/CO_2 is accompanied by NO emission, suggesting the following scheme:

$$CC_f\{O\}\text{–}NO_2 \rightarrow C\{O\}C_f\{O\} + NO \quad (11)$$

$$C\{O\}C_f\{O\} \rightarrow CC_f\{O\} + CO_2 \quad (12)$$

where $CC_f\{O\}$–NO_2 describes the NO_2 containing complexes. The DRIFT spectra support this conclusion by the direct observation of NO_2 complexes that decompose upon heating.

DRIFT analysis gives a solid molecular base for the interpretation of the acceleration of soot oxidation by relatively low amounts of NO_2. For practical applications this calls for a separate catalytic function, viz., the oxidation of NO into NO_2. In the CRT system [24] and recently published paper on the improvements of CRT [25], this is demonstrated.

5. Conclusions

In the soot-NO_2–O_2 reaction system, as in the CRT system, the oxidation of soot is initiated by the NO_2-soot reaction to create SOCs as intermediates. These intermediates are reactive to oxygen, yielding less stable intermediates or they directly produce CO and/or CO_2. As a result, soot oxidation with NO_2 is enhanced by the presence of O_2. This theory is in agreement with soot combustion data.

In NO_2-soot and NO_2/O_2-soot reaction the reactivity of NO_2 and NO_2/O_2 to Printex-U and diesel soot (both idle and full load soot) are similar. With respect to O_2 alone the reactivity of the soot samples is much lower and follows the order of Printex-U < full load soot < idle soot. This order correlates with the hydrogen-content. The reason for the low reactivity is that O_2 only slowly generates SOCs at the low temperature of the exhaust gases. For both soot-O_2 and soot-NO_2 based reaction Printex-U is a reliable soot model that can be used in exploratory studies.

References

[1] R. Allansson, P.G. Blakeman, B.J. Cooper, H. Hess, P.J. Silcock, A.P Walker, SAE Paper 2002-01-0428 (2002).
[2] R. Verbeek, M. van Aken, M. Verkiel, SAE Paper 2001-01-1947 (2001).
[3] PSA PEUGEOT CITROËN/Technology (2001) http://www.psa.fr Accessed August 2003.
[4] K. Itoh, T. Tanaka, S. Hirota, T. Asanuma, K. Kimura, K. Nakatani, US patent, US 6,594,911, assigned to Toyota Motors Ltd. (2003).
[5] H.A. Al-Abadleh, V.H. Grassian, J. Phys. Chem. A. 104 (2000) 11926.
[6] D. Stadler, J. Rossi, Phys. Chem. Chem. Phys. 2 (2000) 5420.
[7] F. Jacquot, V. Logie, J.F. Brilhac, P. Gilot, Carbon 40 (2002) 335.
[8] P.G. Gray, D.D. Do, Chem. Eng. Comm. 117 (1992) 219.
[9] B.A. Lur'e, A.V. Mikhno, Kinet. Catal. 38 (4) (1997) 535.
[10] X. Chu, L.D. Schmidt, Ind. Eng. Chem. Res. 32 (1993) 1359.
[11] J.P.A. Neeft, T.A. Nijhuis, E. Smakman, M. Makkee, J.A. Moulijn, Fuel 76 (1997) 1129.
[12] S.J. Jelles, B.A.A.L. van Setten, M. Makkee, J.A. Moulijn, Appl. Catal. B 21 (1999) 35.
[13] G. Mul, Catalytic diesel exhaust purification—a mechanistic study of soot oxidation. PhD Thesis, TU Delft, 1997.
[14] D.M. Smith, A.R. Chungtai, Colloids Surf. A 105 (1995) 47.
[15] P.E. Fanning, M.A. Vannice, Carbon 31 (5) (1993) 721.
[16] G. Mul, J.P.A. Neeft, F. Kapteijn, J.A. Moulijn, Carbon 36 (9) (1998) 1269.
[17] K.E. Benfell, B.B. Beamish, K.A. Rodgers, Thermochim. Acta 286 (1996) 67.
[18] J.L. Figueiredo, M.F.R. Pereira, M.M.A. Freitas, J.J.M. Orfao, Carbon 37 (1999) 1379.
[19] M.S. Akhter, A.R. Chungtai, D.M. Smith, J. Phys. Chem. 88 (1984) 5334.
[20] S.G. Chen, R.T. Yang, F. Kapteijn, J.A. Moulijn, Ind. Eng. Chem. Res. 32 (1993) 2835–2840.
[21] J.A. Moulijn, F. Kapteijn, Carbon 33 (8) (1995) 1155.
[22] C. Li, T.C. Brown, Carbon 39 (2001) 725.
[23] L.R. Radovic, in: K.H.J. Buschow, R.W. Chahn, M.C. Flemings, B. Ilschner, E.J. Kramer, S. Mahajan (Eds.), Encyclopedia of Materials: Science and Technology, Elsevier, Amsterdam, 2001, p. 975.
[24] B.J. Cooper, J.E. Thoss, SAE Paper 890404 (1989).
[25] A. Setiabudi, M. Makkee, J.A. Moulijn, Appl. Catal. B 42 (2003) 35.